

## **Luminescence Profiling and Flood Sediments from an Arctic Lake Over the Last Millenia**

ANASTASIA POLIAKOVA <sup>1#</sup>, ANTONY G. BROWN <sup>1</sup>, DAVID C.W. SANDERSON <sup>2</sup>, ALAN J. CRESSWELL <sup>2</sup>, LENA M. HÅKANSSON <sup>3</sup>, TOMASZ GOSLAR <sup>4,5</sup>, AND INGER G. ALSOS <sup>1</sup>

---

<sup>1</sup> *The Arctic University Museum, UiT-The Arctic University of Norway, NO-9037 Tromsø, Norway*

<sup>2</sup> *Scottish Universities Environmental Research Centre, Environmental Physics, Rankine Avenue, Scottish Enterprise Technology Park, East Kilbride G75 0QF, UK*

<sup>3</sup> *The University Centre in Svalbard (UNIS), Svalbard Science Centre, P.O. Box 156, NO-9171 Longyearbyen, Norway*

<sup>4</sup> *Adam Mickiewicz University, Faculty of Geographical and Geological Sciences, Rubież 46, 61-612 Poznan, Poland*

<sup>5</sup> *Poznan Radiocarbon Laboratory, Park of Science and Technology, Poznan, Poland*

# *Corresponding author. Phone: +47 77 623 266, E-mail: [anastasia.poliakova@uit.no](mailto:anastasia.poliakova@uit.no)*

### **ABSTRACT**

A small Arctic floodplain-lake (Tendammen, Colesdalen valley) in Svalbard revealed a laminated sediment sequence with numerous <sup>14</sup>C AMS age-depth reversals in its 800 year history. In order to test the hypothesis that the anomalous dates result from catchment erosion and the deposition of reworked sediment and macrofossils, we applied luminescence profiling and flood-sensitive biological proxies. This revealed that many of the dates levels have high portable and laboratory-verified optically and infra-red stimulated luminescence (OSL/IRSL). This is interpreted as resulting from floods delivering partially unbleached sediment-aggregates along with plant macrofossils into the lake. This confirms that luminescence from lake cores can be used to identify flood events from lake sediments, which may often be associated with old carbon from the catchment depending upon catchment history. The flood record generated using a composite age-depth model (SCPs, uplift and selected <sup>14</sup>C dates) is compared with other climate records and supports an increasing climatic variability over the last millennia as rapid warming proceeds in the High Arctic.

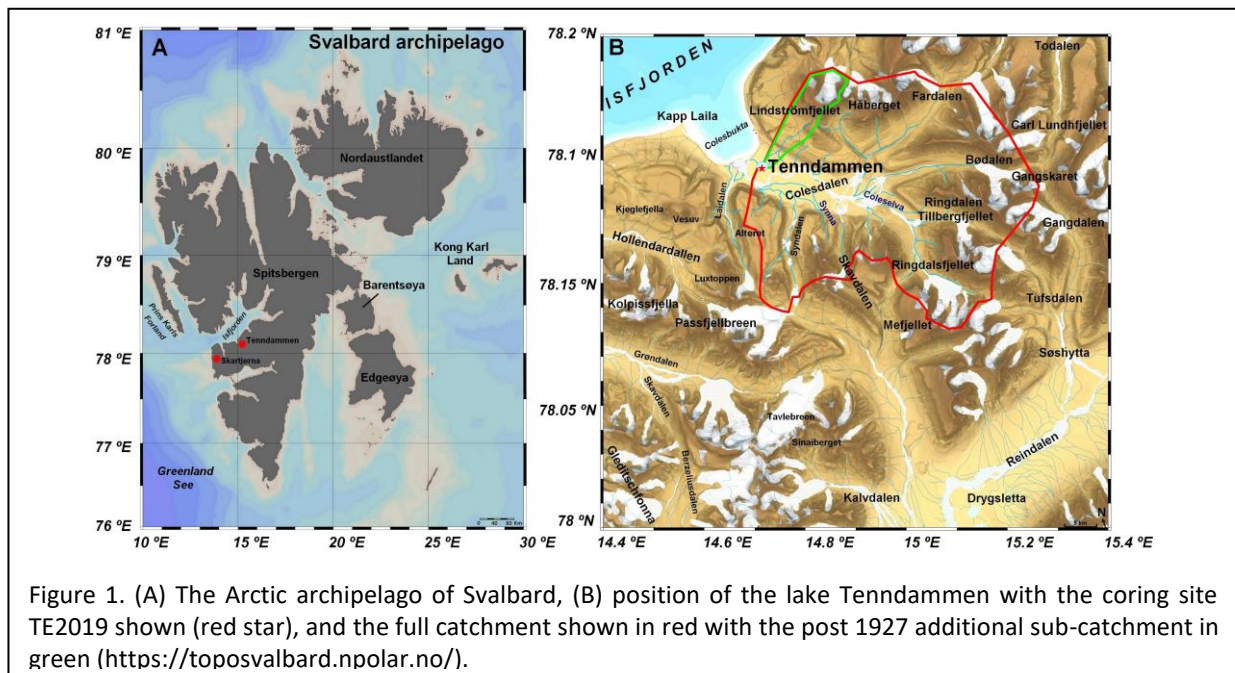
**KEY WORDS:** climate change; flood; lake sediments; late Holocene; portable OSL measurements; Svalbard

## **Introduction**

With the Arctic warming at three times the rate than any other area on Earth understanding links between climate and flooding is urgent (Masson-Delmotte *et al.* 2021; Zhang *et al.* 2022). One of the few records we have of flood-series prior to the instrumented period is the archive of flood-inwashed sediments into lakes as used across Europe including Scandinavia, North America and many other areas (Schillereff *et al.* 2019; Støren and Paasche 2014; Engeland *et al.* 2020; Hsü and Kelts 1985; Baker *et al.* 2021). The methods used to identify flood-sediments including visible stratigraphy, geochemistry and microfossils require an accurate age-depth model in order to produce valid flood-series (Schillereff *et al.* 2019). For periods before the instrumental record (which varies geographically) this is typically 14C. However, a common problem is that 14C dates can be highly scattered (off-sets) and even reversed (older above younger) especially in the lateglacial and later Holocene (Johansson *et al.* 2020; Edwards and Whittington 2001). In the site analysed here we have this problem on an extreme scale with 7 date reversals in a series of 13 dates all within the last millennium. To try and resolve the chronology in order to generate a proxy flood series we investigated the optically and infra-red stimulated luminescence profile (OSL/IRSL) of the sediments in order to reveal zones of likely inwash of partially unbleached sediment and compare them with the raw date series. By doing this, and by applying geomorphological dating derived from relative sea level rise and a strong spheroidal carbonaceous particle profile (SCP) we were able to create a composite age-depth model which we could use to provide a chronology for the flood-series.

## **Methods**

Lake Tenndammen is a small floodplain-lake in the High Arctic archipelago of Svalbard (Spitsbergen, Шпицберген) that has an area of 1,500 m<sup>2</sup> (0.15 ha), a mean depth of 1.5 m and a maximum depth of 2.5 m (Figure 1A). It is located on the valley floor of the Colesdalen valley in Nordenskiöld Land (Figure 1B). Tenndammen receives inputs from floods of the Colesdalelva river but also has a small sub-catchment of 20.5 ± 0.2 km<sup>2</sup> (Figure 1, green line). The Colesdalen catchment is almost entirely unglacierised (<10 % ice) but is entirely periglacial and underlain by Palaeocene-Eocene shale and coal seams with the valley floor covered by marine sediments and fluvio-glacial deposits (Dallman 2015). From historic maps (1910, 1912, 1927 CE and post WWII) it appears that lake Tenndammen was only connected with its western tributary after 1927 probably due to a natural avulsion (Holmsen 1910; Hoen and Staxrud 1927). This stream diversion has helped maintain the water depth used for water supply to the coal mining settlement in Colesbukta before its closure in 1965 CE and reflected in the name “Tenndammen” (*dammen* is dam in Norwegian). Most importantly at a level of 2-2.5 m asl the lake is below the level of the braid-plain of Colesdalelva directly upstream (2.5-3 m asl) and geomorphological observations in September 2022 revealed a number of fresh scour-holes and flood trash between the river and the lake. The geomorphological model used here is based upon the interpretation of aerial photographs, a digital elevation model provided by SvalbardTopo augmented by observations in 2002 and the nearest relative sea level record (RSL)(Landvik *et al.* 1987).



### Core analyses

A core 0.85 m long and 60 mm in diameter core was obtained from the centre of the lake (TE2019, 78.10196°N, 15.03373°E; 5 m asl) in September 2019. The core was lithologically described, photographed, X-ray imaged, line-scanned and X-Ray Fluorescence (XRF) scanned using an Avaatech XRF core scanner. Elemental geochemical profiles for TE2019 from the XRF scanning were used as proxies for variations in depositional conditions (Kylander *et al.* 2011; Löwemark *et al.* 2011). Ratios Fe/Ti, Si/Ti, Al/Si were calculated in order to control grain size fractionation effects, biogenic production within the lake (i.e. biogenic silica) and grain size effects, respectively. Data on the plant proxies, i.e. sedimentary ancient DNA (*sedaDNA*), plant macro-remains and non-pollen microfossils were obtained as it is described in Poliakova *et al.* (in preparation) for Tenndammen and in Alsos *et al.* (2016) for Skartjørna. Loss of ignition method (LOI) was applied to estimate organic content of the sediments following the standard procedure (Heiri *et al.* 2001).

### Luminescence profiling and measurements

Luminescence profiling was undertaken using the portable unit developed by the Scottish Universities Environmental Research Centre (SUERC) for complex and heterogeneous sediment sequences (Sanderson *et al.* 2010). Assuming that day light only penetrates *c.* 2-4 mm into fine high-density sediments (Alexanderson and Murray 2012) and taking into account that XRF X-rays scanners can affect about 5 mm below the surface (Davids *et al.* 2012), samples were taken from the inner part of the intact and dark-kept core half (depth *c.* 2-2.5 cm), air-dried, homogenized and dispersed to 50 mm petri dishes in preparation for portable luminescence measurement. All sample handling was conducted under weak red light to reduce potential optical bleaching of the samples. Measuring protocol and following calculations are available in the Supplementary materials (Methods) for pOSL/pIRSL measuring protocol and pOSL and pIRSL calculations. Measured values of XRF, LOI, pIRSL and pOSL as well as their ratios (pIRSL/pOSL) are given in the Fig. 3. To perform a control on the mineralogical composition in the sediments, depletion indices (IRdep, OSLdep) were additionally calculated.

Luminescence sensitivities, sensitivity changes and stored doses (Gy) were evaluated from the paired aliquots of the polymineral and HF-etched quartz fractions, using a Risø DA-20 automatic reader equipped with a  $^{90}\text{Sr}/^{90}\text{Y}$   $\beta$ -source for irradiation, using blue LEDs emitting around 470 nm (OSL) and infrared (laser) diodes emitting around 830 nm (IRSL) for optical stimulation, and a U340 detection filter pack to detect in the region 270-380 nm. For quartz, each measurement was preceded by a pre-heat at 200°C for 10s, with a 30s OSL measurement at 125°C. Measurements were conducted for the natural signal, and following nominal 5 Gy and 50 Gy irradiations, with all measurements accompanied by a nominal 1 Gy test dose. For the polymineral samples, each measurement was preceded by a pre-heat at 200°C for 10s, with a 30s IRSL measurement at 50°C, a 30s OSL measurement at 125°C and a TL measurement to 500°C. Measurements were conducted for the natural signal and following nominal 5 Gy and 50 Gy irradiations. Details on the IRSL and OSL measurements for the residual luminescence dose are given in the Supporting Information Table 1.

## **Results and interpretation**

### **Geomorphology and age constraints**

Mapping of terraces, palaeochannels and raised beach ridges along with the nearest relative sea level curve (Landvik *et al.* 1987) has allowed a model of the evolution of the lake and its isolation due to RSL fall (Fig. 2). The RSL and geomorphology indicates that the lake must have been isolated between 1000 and 700 years over this period it must have received flood inputs whenever the Colesdalelva went overbank at the braided channel inflection point 400 m to the south-east of the lake. This suggests that the two basal dates which statistically overlap at the 1 sigma probability do reflect the true age of the basal sediments and are reliable age-depth points.

### **Lithostratigraphy and age-depth modelling**

The core TE2019 revealed a laminated sequence of peaty silts and peaty silts with LOI varying between 1% and 8% by dry weight (Fig. 3). The sequence was divided into five stratigraphic units based upon the main sediment type (Fig. 3). However, all the units contained thin sediment laminations formed by micro-fining upwards grain-size and increase in organic matter at a scale of 5-10 mm. In all 85 laminations could be counted but this is almost certainly an underestimate of floods due to disturbance in the basal units (unit 1 and 2) and more massive sediments in units 4 and 5. It is also possible that single floods could have deposited multiple laminations due to flood pulses during a major snow-melt driven hydrograph.

Despite the extraction of identified terrestrial macrofossils (Table 1) 10 out of 13 dates were reversed with age-inversions (dated aging upwards) (Fig. 4). However, the upper 0.275 m of sediments produced a coherent spheroidal carbonaceous particles (SCP) profile. This profile corresponds with the calendar ages of the history of the coal mining and power production in Svalbard, and provided three tie points at the age-depth model, related to (1) construction of the power plant in 1911-1913 in Colesdalen, (2) abrupt decrease in SCP associated with the Second World War 1941-1946, and (3) the highest output of the power plant in Colesdalen during 1950-80s. It also corresponds to the model derived from heavy metals by Boyle (2004). This allowed a best-fit composite model to be generated using the lower non-reversed dates and the upper SCP model (Fig. 3). A second constraint used for the model is an estimated basal date based upon the closest sea-level curve, from the same peninsular (Nordenskiöldkysten) 30 km to the west (Landvik *et al.* 1987). This provides an estimated date for the abandonment of the Colesdalen embayment which created the lake which was 1000-700 years ago and agreed with the two statistically overlapping basal  $^{14}\text{C}$  dates. The other dates used were selected on the basis of the pOSL/pIRSL profile.



Fig. 2 a. **a-d** A geomorphological model of the evolution of Tenndammen lake based on maps, field observations and RSL, **e** peat balls at the edge of the lake 2020, **f** bank tension cracks at the inflection and spill-over point of the Colesdalen river (2020).

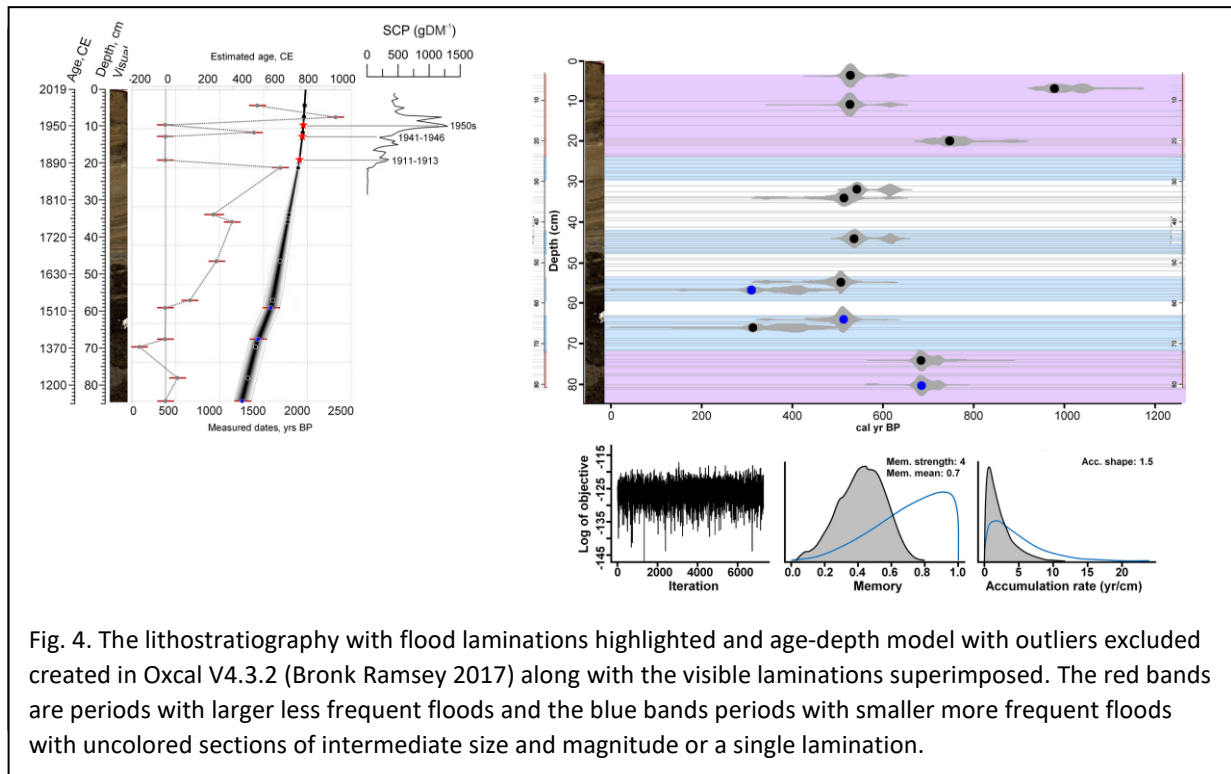
The composite age-depth model has been created using only the consistent dates at the base and backward interpolation of the SCP model.

Depth (cm)	Laboratory ID	14C age	Cal. W. mean	Cal. median	Cal. 2σ range	Sample contents
4.0	Poz-121134	500 ± 30	1395	1450	1399 - 1450	Moss ( <i>Caliergon</i> , <i>Warnstorfia</i> )
7.0	Poz-121135	1095 ± 30	924	1017	890 - 1017	Moss ( <i>Caliergon</i> , <i>Warnstorfia</i> )
9.0				1912	1911 - 1913	SCP
11.0	Poz-121136	505 ± 30	1393	1450	1396 - 1450	Moss ( <i>Caliergon</i> , <i>Warnstorfia</i> )
12.0				1944	1941 - 1946	SCP
18.0				1955	1951 - 1958	SCP
20.0	Poz-112299	845 ± 30	1183	1267	1159 - 1267	Moss ( <i>Caliergon</i> , <i>Warnstorfia</i> )
32.0	Poz-121138	550 ± 30	1472	1607	1397 - 1607	Moss ( <i>Caliergon</i> , <i>Warnstorfia</i> )
34.0	Poz-123841	470 ± 40	1336	1434	1318 - 1434	<i>Salix polaris</i> leaves
44.0	Poz-121139	535 ± 30	1351	1439	1323 - 1439	Moss ( <i>Caliergon</i> , <i>Warnstorfia</i> )
54.0	Poz-112300	445 ± 30	1423	1490	1416 - 1490	Moss ( <i>Caliergon</i> )
56.0	Poz-123842	290 ± 30	1551	1662	1499 - 1662	<i>Salix polaris</i> leaf fragments
64.0	Poz-112301	460 ± 30	1412	1471	1412 - 1471	Moss ( <i>Caliergon</i> )
66.0	Poz-123843	305 ± 30	1543	1653	1492 - 1653	<i>Salix polaris</i> leaf fragments
74.0	Poz-112302	760 ± 30	1224	1285	1222 - 1285	Moss ( <i>Caliergon</i> , <i>Warnstorfia</i> )
80.0	Poz-112303	755 ± 30	1226	1288	1224 - 1288	Moss ( <i>Caliergon</i> , <i>Warnstorfia</i> )

Table 1. Radiocarbon dates from Lake Tenndammen (core TE2019) with the addition of SCP tie points.

### **Plant proxies and flood laminations**

The full results of the palaeoecological analyses are given in Poliakova (Subm.) but in summary macrofossil analysis produced a total of 91 vascular plant taxa along with 65 bryophyte taxa and 3 types of algal cells. The pattern of occurrence corresponded to variation in the lithology with peaks in the semi-aquatic moss *Warnstorfia exannulata/Warnstorfia fluitans* macrofossils and algal cells associated with stratigraphically marked flood events in units L1-L3. This was accompanied by *sedaDNA* of the freshwater algae, i.e. *Closterium littorale*, *Cosmarium botrytis*, *Staurastrum punctulatum* and *Nannochloropsis* sp. (Fig. 3). In contrast, eight samples had no or minimal aquatic bryophytes and algae. From a combination of the laminations, the plant macrofossils, the aquatic *sedaDNA* and the presence of algal cells an interpretation was made of flood events prior to luminescence profiling.



#### Luminescence profiling and dose rate verification

At Tenndammen both pIRSL and pOSL showed unexpectedly large variations up core with pIRSL intensity varying from a minimum of 332 photons to a maximum of c. 98,000 photons with an average of c.  $16,000 \pm 180$  photons. Likewise, pOSL varied from minima of 12,000 to 419,000 photons with a mean of  $97,000 \pm 800$  photons (Fig. 5). It is also noticeable that the variation is in the form of distinct positive peaks falling well outside the standard deviation of the distribution. Minima in the pIRSL correspond to minima in the pOSL, and likewise for the maxima as reflected in the ratio pIRSL/pOSL which only varies between 0.1 and 0.3, with a small number of large excursions to very low (minimum 0.005) or very high (maximum 1.25) values, with the average of  $0.15 \pm 0.1$ . These ratios can be related to proportions of quartz and feldspar minerals in the samples and the signals each of them produce. Whereas the relative contribution of faster and slower signals (depletion indices IRdep and OSLdep, respectively; Fig. 5) often interpreted as relating to the proportion of residual signals, do not change significantly.

In order to verify the pIRSL and pOSL measurements, 3 samples from laminae (assumed flood events) and 3 samples with anomalous low values were analysed using a laboratory profiling method (Sanderson *et al.* 2003, 2007; Burbidge *et al.* 2007) applied to 10-60  $\mu\text{m}$  polymineral and 10-20  $\mu\text{m}$  nominal quartz grains. Luminescence sensitivities, sensitivity changes and stored doses (Gy) were performed. This verifies that the samples with low signals from the portable instrument (at 7.5, 47.5 and 78.0 cm; Supporting Information, Fig. 3) also produce low signals from the polymineral fraction, the sample with the highest signals from the portable instrument also gives the highest signals from the polymineral fraction. The other

two samples give elevated polymineral signals, but not in proportion to the signals observed with the portable instrument.

Four of the quartz fraction measurements represent higher OSL signals, not correlated with the polymineral or portable measurements (Supporting Information Fig. 1), probably reflecting the low quartz content of the samples resulting in small contributions to the bulk sample measurements. The samples with the lower portable measurements signals also produce lower counts in the laboratory analysis, with apparent doses in the 5-10 Gy range, which would correspond to apparent ages of 2-4 ka assuming dose rates typical of average crustal radionuclide concentrations. The results are consistent with floods moving minerals in turbid conditions with limited exposure to daylight, and thus not removing residual signals before deposition on the lake bed, and for significantly greater exposure to day light during the intervening episodes. The very low values (in one case near 0) imply the partial bleaching of these sediments which could have happened through resuspension of fine sediment caused by wind and/or lowered lake levels or an aeolian input. Although dust storms are not uncommon in Svalbard (Rymer 2018) in-situ bleaching is probably the most likely as neither the LOI or XRF suggest distinctive fine sand laminations typical of dust-storms.

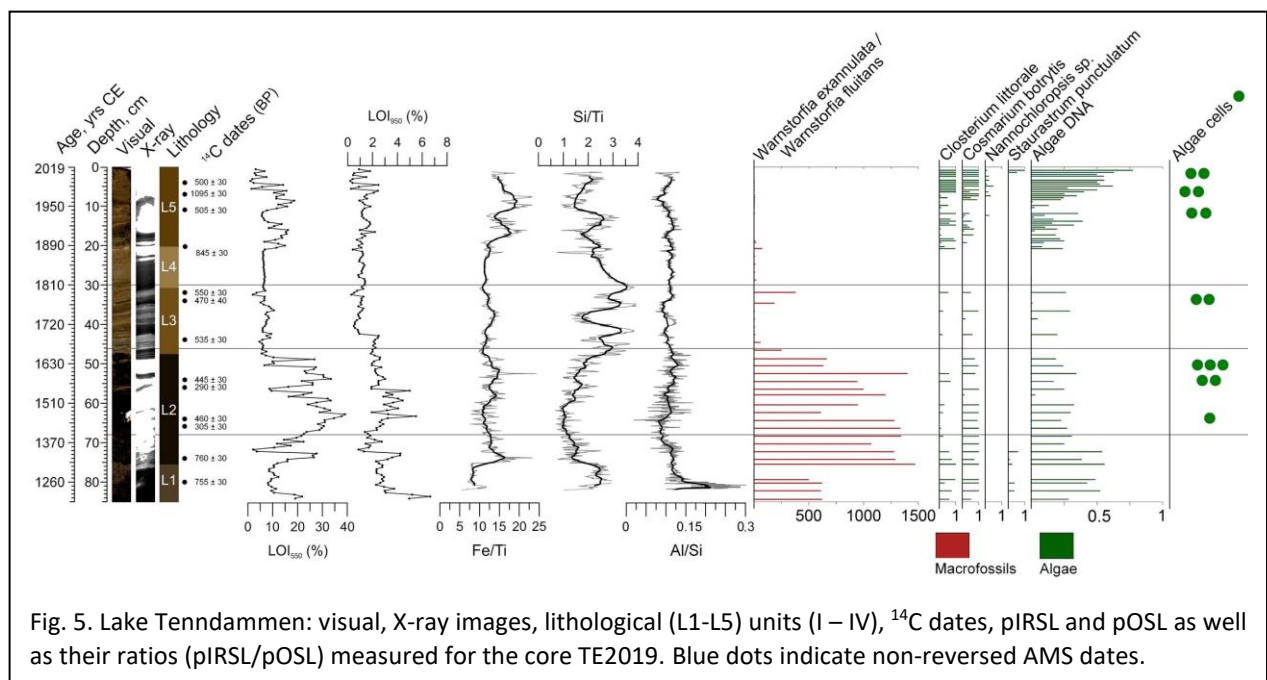


Fig. 5. Lake Tenndammen: visual, X-ray images, lithological (L1-L5) units (I – IV), <sup>14</sup>C dates, pIRSL and pOSL as well as their ratios (pIRSL/pOSL) measured for the core TE2019. Blue dots indicate non-reversed AMS dates.

### Discussion: flood and climate history of Svalbard

The pIRSL, pOSL and pIRSL/pOSL profiles at Tendammen show minimal values (c. 500 photons and lower) at 8 levels which suggests bleaching of the sediments and these minima are in most cases succeeded by very high values (maximal c. 98,000 photons with average being c. 16,000 ± 180 photons in pIRSL, and to maximal of 419,000 photons with the average of 97,000 ± 800 photons in pOSL). When compared to the plant macrofossils, the luminescence record corresponds with periods when the lake appears to have received old material from the soil surface and river banks due to erosion in the catchment, and periods when the sediment was

partially-bleached. Indeed reworked organic materials in the form of peat-balls were observed in the lake in 2022 (Fig. 2e) and evidence of erosion at the edges of the braid-plain immediately upstream of the lake (Fig. 2f). The old sediment is unlikely to have come from the glaciers located in the lake catchment as Alexanderson and Murray (2012) have shown that these are fully bleached by travelling 3 km away from the glacier. Although the laminations record at least 85 events we can see approximately 15 events from the pOSL/pIRSL and proxies in the lakes 800 year history.

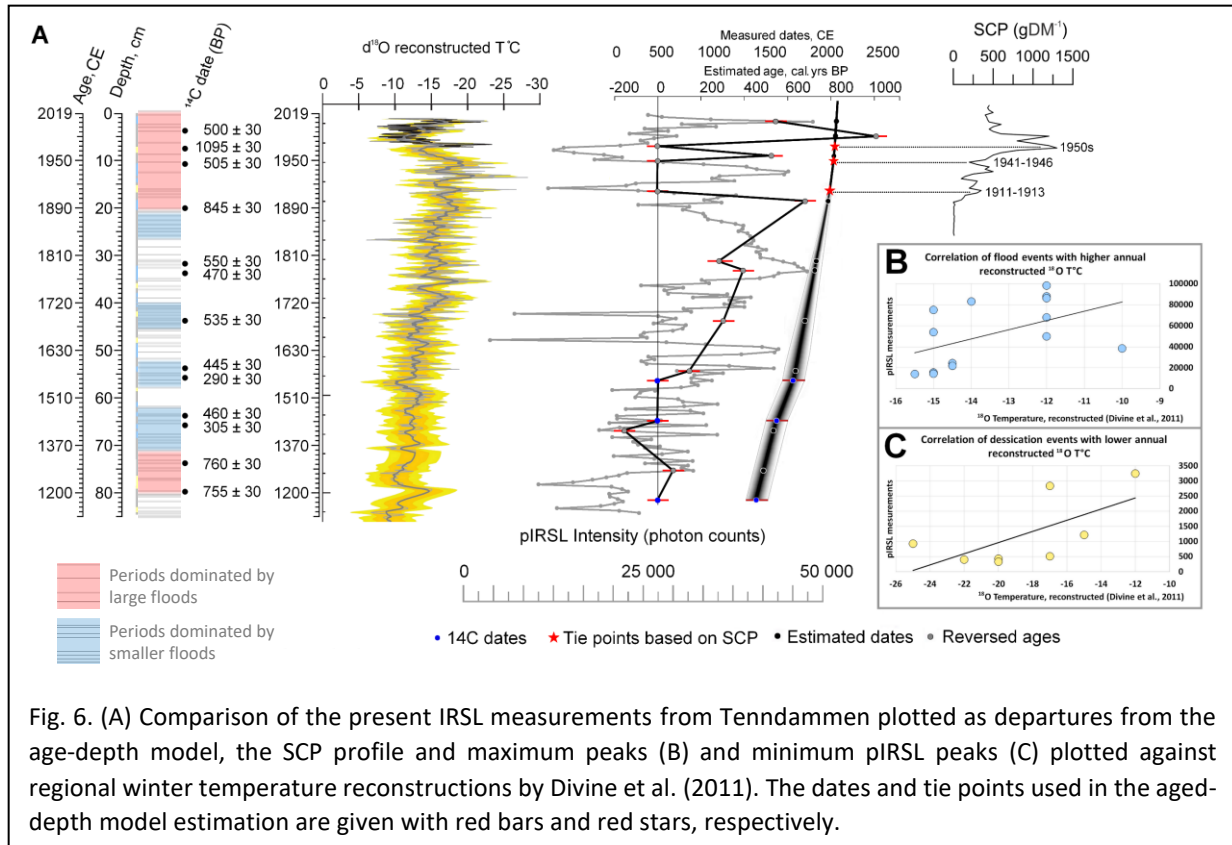


Fig. 6. (A) Comparison of the present IRSL measurements from Tenndammen plotted as departures from the age-depth model, the SCP profile and maximum peaks (B) and minimum pIRSL peaks (C) plotted against regional winter temperature reconstructions by Divine et al. (2011). The dates and tie points used in the aged-depth model estimation are given with red bars and red stars, respectively.

Although Tenndammen has acted as a trap for flood sediments from the Colesdalen river over the last 800 years it is not possible to directly generate a full flood-series from the sequence due to; a) the probable changing elevation of the main river and so changing return interval of overbank flows, b) non-stationary relationships between flood magnitude and sediment load, and c) remaining dating uncertainties. As there is unlikely to have been significant loss of sediment from the lake through the small and discontinuous outlet channel, sediment input lead to an increasing incidence of lake shallowing and drying out. Today the lake can be shallow (under 1m) and is frequently highly turbid due to sediment resuspension. An important factor is the catchment's complex and inherently erodible geology which is Palaeocene–Eocene sandstone, shale, and coal seams covered by Holocene aeolian sediments and weathering products. This rock-pile produces high suspended sediment concentrations, almost certainly with high levels of aggregation due to high clay and organic matter.

In order to test a correlation between the pIRSL record and climate we used the  $\delta^{18}\text{O}$  derived winter temperatures from Lomonosovfonna and Holtedahlfonna (Divine *et al.* 2011). Although not a direct climate driver of floods the reconstructed winter temperature is strongly

correlated with both mean annual temperature and sea ice extent (Førland *et al.* 2011) and so can mark periods of climatic change including overall warming in the last 100 years (Divine *et al.* 2011). In general, the temperature profile reconstructed for December-February on the  $\delta^{18}\text{O}$  data is reflected in the TE2019 core: higher annual temperatures occur at about the same time with the pIRSL values which should be connected with the intensification of the ice and/or snow melting. At c. 1200-1360 CE and 1890-2019 CE the record was dominated by large floods whereas the periods 1360-1500 CE, 1660-1720 CE and 1830-1890 CE were dominated by smaller floods (Fig. 6A). Correlation of the floods and the reconstructed temperature increase is 0.75 – 0.89 ( $p>95$ ; STD 0.17; Fig. 6B). Inter-flood samples do not show clear correlation with the temperature decrease (0.56 with  $p>95$ ; STD 0.46. Figure 5C).

## **Conclusions**

The luminescence data from floodplain lake Tenndammen confirms that this methodology, which has been used on anthropogenic fluvial pond-sediments (Bishop *et al.* 2011) and Lake Sugetso (Rex *et al.* 2022) can, in the absence of other drivers, reveal reworked sediment brought in by flood events. This allows  $^{14}\text{C}$  date reversals to be seen as potentially valuable data, rather than only dating ‘errors’. The pOSL and pIRSL record from Lake Tenndammen shows a series of floods and flood-rich periods in the last 700 years which includes periods of flood-poor and possibly drought dominance in the Medieval period (c. 1200-1500 CE) and larger floods in the Little Ice Age associated with the maximum Holocene extent of the glaciers (Svendsen 1997) around 13th or 14th century (Werner 1993; Van der Bilt and Bakke 2017; Røthe 2015) and continuing into the last century. The novel methodology outlined here along with other palaeohydrological techniques has the potential to reveal unrecognized climatic events in archive cores, which may facilitate a deeper understanding of climatic instability under changing global forcing.

*Acknowledgments.* We thank The University Centre in Svalbard (UNIS) for logistics support, and Charlotta Sandmo for transportation. Marie Kristine Førleid Merkel (UiT Museum, Tromsø) gets our gratitude for assistance in the DNA laboratories, Martin Hajman and Arve Elvebakk for help with plant remain identifications. Anders Schomacker (Geological department of UiT, Tromsø) is acknowledged for his assistance in the organizing a fieldwork, for his valuable comments on the manuscript and discussions. Trina Merete Dahl gets our regards for technical support in the XRF, and Ingvild Hald for assistance in grain size analysis. This study has been carried out within the international multidisciplinary program “Future Arctic Ecosystems (FATE): drivers of diversity and future scenarios from ethnoecology, contemporary ecology and ancient DNA” (<https://www.fate-biodivscen.org>) and “Ancient DNA of NW Europe reveals responses to climate” (AfterIce) projects.

*Funding.* The research was financially supported by the Research Council of Norway and Biodiversa (grant nos. 213692/F20, 230617/E10, and 296987/E50).

## **Supporting information**

Online file

## **References**

Alexanderson, H., Murray, A.S. 2012. Luminescence signals from modern sediments in a glaciated bay, NW Svalbard. *Quaternary Geochronology* **10**: 250 – 256.

Alsos, I.G., Sjögren, P., Edwards, M., Landvik, J., Gielly, L., Forwick M., Cossack, E., Brown, A.G., Jacobsen, L. V., Føreid, M., Pedersen, M. 2016. Sedimentary ancient DNA from Lake Skartjørna, Svalbard: Assessing the resilience of arctic flora to Holocene climate change. *The Holocene* **26**: 627 – 642 (2016).

Baker, V.R., Benito, G., Brown, A.G., Carling, P.A., Enzel, Y., Greenbaum, N., Herget, J., Kale, V.S., Latrubesse, E.M., Mackling, M.G., Nanson, G., Oguchi, T., Thorndycraft, V.R., Ben Dor, Y., Zituni, R. 2021. Fluvial palaeohydrology in the 21st century and beyond. *Earth Surface Processes & Landforms* **2021**: 1-24.

Bishop, P., Muñoz-Salinas, E., MacKenzie, A.B., Pulford, I., McKibbin, J. 2011. The character, volume and implications of sediment impounded in mill dams in Scotland: the case of the Baldernock Mill dam in East Dunbartonshire. *Earth and Environmental Science Transactions of the Royal Society of Edinburgh* **101**: 97 – 110.

Boyle J.F., Rose N.L., Appleby P.G., Birks H.J.B. 2004. Recent environmental change and human impact on Svalbard: the lake-sediment geochemical record. *Journal of Paleolimnology* **31**: 515 – 530.

Bronk Ramsey, C. 2017. Methods for Summarizing Radiocarbon Datasets. *Radiocarbon* **59**: 1809 – 1833.

Burbidge, C.I., Sanderson, D.C.W., Housley, R.A., Allsworth Jones, P. 2007. Survey of Palaeolithic sites by luminescence profiling, a case study from Eastern Europe. *Quaternary Geochronology* **2**: 296 – 302.

Divine D., Isaksson E., Martma T., Meijer H. A., Moore J., Pohjola V., van de Wal R. S., Godtlielsen F. 2011. Thousand years of winter surface air temperature variations in Svalbard and northern Norway reconstructed from ice-core data. *Polar Research* **30**: 7379.

Chiverrell, R.C., Sear, D.A., Warburton, J., Macdonald, N., Schillereff, D.N. Dearing, J.A., Croudace, I.W., Brown, J., Bradley, J. 2019. Using lake sediment archives to improve understanding of flood magnitude and frequency: recent extreme flooding in northwest UK. *Earth Surface Processes and Landforms* **44**: 2366–2376.

Dauids, F., Roberts, H. M. & Duller, G. A. T. 2010. Is X-ray core scanning non-destructive? Assessing the implications for optically stimulated luminescence (OSL) dating of sediments. *Journal of Quaternary Science* **25**: 348 – 353.

Engeland, K., Aano, A., Steffensen, I., Støren, E., Paasche, Ø. 2020. New flood frequency estimates for the largest river in Norway based on the combination of short and long time series. *Hydrol. Earth System. Science* **24**: 5595-5619.

Heiri, O., Lotter, A.F., Lemcke, G. 2001. Loss on ignition as a method for estimating organic. *Journal of Paleolimnology* **25**: 101 – 110.

Holmsen, G. 2010. *Skizze des Gebietes zwischen Belsund und Eisfjorden (Süd-Spizbergen)*. Karte 1:275.000, Gotha.

Hoen, A., Staxrud, A. 1927. *Svalbard (Spitsbergen) boundary map of the area*. N20 (1: Colesbukta). Map 1:50,000, Oslo.

- Johansson, F. E., Bakke, J., Støren, E. N., Paasche, Ø., Engeland, K., Arnaud, F. 2020. Lake Sediments Reveal Large Variations in Flood Frequency Over the Last 6,500 Years in South-Western Norway. *Frontiers in Earth Sciences* **8**: 239.
- Landvik, J.Y., Mangerud, J. & Salvigsen, O. 1987. The Late Weichselian and Holocene shoreline displacement on the west-central coast of Svalbard. *Polar Research* **5**: 29 – 44.
- Masson-Delmotte, V., et al. 2021. *Climate Change 2021: The Physical Science Basis. Contribution of Working Group I to the Sixth Assessment Report of the Intergovernmental Panel on Climate Change*. Cambridge University Press.
- Rex, C.L., Staff, R.A., Sanderson, D.C.W., Cresswell, A.J., Marshall, M.H., Hyodo, M., Horiuchi, D., Tada, R., Nakagawa, T. 2022. Controls on luminescence signals in lake sediment cores: A study from Lake Suigetsu, Japan. *Quaternary Geochronology* **71**: 101319.
- Røthe, T.O. 2015. Arctic Holocene glacier fluctuations reconstructed from lake sediments at Mitrahavøya, Spitsbergen. *Quaternary Science Reviews* **109**: 111 – 125.
- Rymer, K. Aeolian activity in central Spitsbergen (Ebba Valley) in the years 2012-2017. 2018. XXXVII *Symposium Polarne Polar Change – Global Change*, 7-10 June, Poznan, p. 612018.
- Sanderson, D.C.W., Murphy, A. 2010. Using simple portable OSL measurements and laboratory characterization to help understand complex and heterogeneous sediment sequences for luminescence dating. *Quaternary Geochronology* **5**: 299 – 305.
- Sanderson, D.C.W., Bishop P., Stark, M.T., Spencer, J.Q. 2003. Luminescence dating of anthropologically reset canal sediments from Angkor Borei, Mekong Delta, Cambodia. *Quaternary Science Reviews* **22**: 1111 – 1121.
- Sanderson, D.C.W., Bishop, P., Stark, M., Alexander, S., Dan Penny, D. 2007. Luminescence dating of canal sediments from Angkor Borei, Mekong Delta, Southern Cambodia. *Quaternary Geochronology* **2**: 322 – 329.
- Schillereff, D.N., Chiverrell, R.C., Macdonald, N., Hooke, J.M. 2014. Flood stratigraphies in lake sediments: A review. *Earth-Science Reviews* **135**: 17–37.
- Støren, E. N., Paasche, Ø. 2014. Scandinavian floods: from past observations to future trends. *Global and Planetary Change* **113**: 34-43.
- Svendsen, J. I., Mangerud, J. 1997. Holocene glacial and climatic variations on Spitsbergen, Svalbard. *The Holocene* **7**: 45 – 57.
- Van der Bilt, W., Lane, C., Bakke, J. 2017. Ultra-distal Kamchatkan ash on Arctic Svalbard: Towards hemispheric cryptotephra correlation. *Quaternary Science Reviews* **164**: 230 –235.
- Werner, A. 1993. Holocene moraine chronology, Spitsbergen, Svalbard: lichenometric evidence for multiple Neoglacial advances in the Arctic. *The Holocene* **2**: 128 – 137.
- Zhang, T., Dongfeng, T.Z., East, A.E., Walling, D.E., Lane, S., Overeem, I., Beylich, A.A., Lu, X. 2022. Warming-driven erosion and sediment transport in cold regions. *Nature Reviews Earth & Environment* **3**: 832-851.